



Since January 2020 Elsevier has created a COVID-19 resource centre with free information in English and Mandarin on the novel coronavirus COVID-19. The COVID-19 resource centre is hosted on Elsevier Connect, the company's public news and information website.

Elsevier hereby grants permission to make all its COVID-19-related research that is available on the COVID-19 resource centre - including this research content - immediately available in PubMed Central and other publicly funded repositories, such as the WHO COVID database with rights for unrestricted research re-use and analyses in any form or by any means with acknowledgement of the original source. These permissions are granted for free by Elsevier for as long as the COVID-19 resource centre remains active.



Heme oxygenase-1(HO-1) regulates Golgi stress and attenuates endotoxin-induced acute lung injury through hypoxia inducible factor-1 α (HIF-1 α)/HO-1 signaling pathway

Xiangyun Li^{a,1}, Jianbo Yu^{a,*}, Lirong Gong^{a,1}, Yuan Zhang^a, Shuan Dong^a, Jia Shi^a, Cui Li^a, Yuting Li^a, Yanfang Zhang^a, Haibo Li^b

^a Department of Anesthesiology and Critical Care Medicine, Tianjin NanKai Hospital, Tianjin Medical University, Tianjin, China

^b Department of Anesthesiology, Chifeng Municipal Hospital, Inner Mongolia, China

ARTICLE INFO

Keywords:

Acute lung injury
Golgi stress
Heme oxygenase-1
Oxidative stress

ABSTRACT

Sepsis caused acute lung injury (ALI) is a kind of serious disease in critically ill patients with very high morbidity and mortality. Recently, it has been demonstrated that Golgi is involved in the process of oxidative stress. However, whether Golgi stress is associated with oxidative stress in septic induced acute lung injury has not been elucidated. In this research, we found that lipopolysaccharide (LPS) induced oxidative stress, apoptosis, inflammation and Golgi morphology changes in acute lung injury both in vivo and in vitro. The knockout of heme oxygenase-1(HO-1) aggravated oxidative stress, inflammation, apoptosis and reduced the expression of Golgi matrix protein 130 (GM130), mannosidase II, Golgi-associated protein golgin A1 (Golgin 97), and increased the expression of Golgi phosphoprotein 3 (GOLPH3), which caused the fragmentation of Golgi. Furtherly, the activation of hypoxia inducible factor-1 α (HIF-1 α)/HO-1 pathway, attenuates Golgi stress and oxidative stress by increasing the levels of GM130, mannosidase II, Golgin 97, and decreasing the expression of GOLPH3 both in vivo and in vitro. Therefore, the activation of HO-1 plays a crucial role in alleviating sepsis-induced acute lung injury by regulating Golgi stress, oxidative stress, which may provide a therapeutic target for the treatment of acute lung injury.

1. Introduction

The Golgi apparatus acts as an important part of the endomembrane system and exists in all eukaryotic cells. In most higher eukaryotic cells, the Golgi consists of a series of flattened cisternae organized into ribbon-like stacks that are closely arranged to each other [1]. These interconnected highly organized stacks of cisternae play a crucial role in the secretory and the endocytic pathways [2]. The maintenance of Golgi organization depends on the large coiled-coil proteins which are known as ‘golgins’ [3]. These glogins include a variety of members, such as GM130, Golgin-160, Giantin and others, which are necessary for vesicular transport, and the maintenance of Golgi structure. It has been demonstrated that Golgi complex is relevant to the ion homeostasis, cell apoptosis, antioxidation, and stress sensing [4]. The integrated structure and steady function of Golgi apparatus could be impaired under oxidative stress, DNA damage and pro-apoptotic conditions, which may

even induce Golgi fragmentation and cell apoptosis [5,6]. Therefore, the Golgi complex has become a new candidate for the research and therapy about oxidative stress-associated diseases.

Sepsis-induced acute lung injury (ALI) is recognized as life-threatening diseases that can aggravate to more severe acute respiratory distress syndrome (ARDS) [7,8]. Since the pandemic of coronavirus disease 2019(COVID-19), about 5% patients with COVID-19 progress to ARDS, septic shock and/or multiple organ failure [9,10]. Therefore, more and more research are focusing on the treatment of acute lung injury or ARDS. Nowadays, it has been demonstrated that septic lung injury associated with a lot of organelles dysfunction. For example, sepsis induced acute lung injury and ARDS is related to the disruption of mitochondrial dynamics and enhanced endoplasmic reticulum stress [11,12]. However, whether acute lung injury can induce the dysfunction and fragmentation of Golgi has not been certified. Therefore, we hypothesized that LPS could induce Golgi stress by disturbing the morphology homeostasis in vivo and in vitro.

* Corresponding author.

E-mail address: yujianbo11@126.com (J. Yu).

¹ These authors contributed equally to this work.

<https://doi.org/10.1016/j.freeradbiomed.2021.01.028>

Received 6 July 2020; Received in revised form 13 January 2021; Accepted 14 January 2021

Available online 23 January 2021

0891-5849/© 2021 Elsevier Inc. All rights reserved.

Abbreviations

| | |
|----------------|---|
| HO-1 | Heme oxygenase-1 |
| HIF-1 α | Hypoxia inducible factor-1 α |
| ALI | Acute lung injury |
| ARDS | Acute respiratory distress syndrome |
| COVID-19 | Coronavirus disease 2019 |
| LPS | Lipopolysaccharide |
| BALF | Bronchoalveolar lavage fluid |
| IL-6 | Interleukin 6 |
| ROS | Reactive oxygen species |
| PBS | Phosphate-buffered saline |
| HE staining | Hematoxylin and eosin staining |
| SOD | Superoxide dismutase |
| DMOG | Prolyl hydroxylase inhibitor dimethylallylglycine |
| PHD | Prolyl hydroxylase |
| COPD | Chronic obstructive pulmonary disease |

Heme oxygenase-1, a stress inducible protein, play an critical effect on signaling and cytoprotective activities in different organs and tissues, as well as its degradation product carbon monoxide (CO), biliverdin and iron [13]. Recently, many studies have shown that HO-1 is involved in maintaining the homeostasis of organelles in cells, such as mitochondria, endoplasmic reticulum and so on [14,15]. Our previous research has demonstrated that HO-1 protect cells from inflammation and oxidative stress by improving mitochondrial dynamics in endotoxin induced acute lung injury in vivo and in vitro [12,16–18]. However, the function of HO-1 on Golgi stress has not been studied. Therefore, in this study, we aimed to identify the relationship between HO-1 and Golgi stress and their mechanisms in LPS-induced ALI.

Hypoxia inducible factors is involved in the cellular adaptation to hypoxia conditions, which conclude HIF- β subunit and HIF- α subunit (HIF-1 α , HIF-2 α , or HIF-3 α) [19,20]. HIF- β is constitutively expressed, while HIF- α is stabilized under hypoxic conditions [21]. HIF-1 α is one of the primary regulators, which binds to hypoxia-responsive enhancer elements (HREs) with its cofactors, and promotes the transcription of multiple genes [22]. Some pro-inflammatory cytokines, a variety of infections and growth factors stimulate the expression of HIF-1 α [22]. HO-1 is one of downstream molecules of HIF-1 α , and it is transcriptionally regulated by HIF-1 α under hypoxia conditions [23]. It has been found that the activation of HIF-1 α /HO-1 signaling pathway ameliorates LPS-induced acute lung injury and protects septic myocardial injury by increasing survival rate, attenuating inflammation, and suppressing oxidative stress [24,25]. However, the role of HIF-1 α /HO-1 on Golgi stress in LPS-induced acute lung injury has not been demonstrated. Therefore, we tried to explore their relationships in sepsis-induced acute lung injury in this study.

2. Materials and methods

2.1. Reagents

LPS (Escherichia coli, O55:B5) were purchased from Sigma (MO, USA). Lipofectamine RNAiMAX Reagent was bought from Invitrogen. The mouse lung epithelial cell line MLE12 were bought from American Type Culture Collection (Manassas, VA, USA). Methyl thiazolyl tetrazolium (MTT) and 2'-7'-dichlorofluorescein diacetate (2'-7'-DCFH-DA) were purchased from (Beyotime Institute of Biotechnology, Nanjing, China). Dimethyl sulfoxide (DMSO, Sigma-Aldrich, USA), Dimethylallylglycine (DMOG, Santa Cruz, USA).

2.2. Animals

Animals: C57BL/6 mice (aged 6–8 weeks, weighing 20–22g, Male) were purchased from Acute Abdominal Diseases of Integrated Traditional Chinese Western Medicine. Experiments were preapproved by the Institutional Animal Use and Care Committee of Tianjin Nankai Hospital, Tianjin, China. HO-1 conditional knockout mice (HO-1^{fl/fl}/CAG-CreERT2) and CAG-iCreERT2 mice were generated by Beijing Biocytogen Co., Ltd. We used Tamoxifen to induce conditional knockout of HO-1 in these mice. The whole strain name of CAG-iCreERT2 mice is C57BL/6-Gt (ROSA)26ortm6(CAG-iCre/ERT2)/Bcgen. An CAG-iCreERT2-WPRE-pA cassette was placed between the exon 1 and exon2 with C57BL/6 embryonic stem cells. This mouse line was maintained on a C57BL/6 genetic background. This CAG-iCreERT2 model is an efficient tool to study different gene functions when crossed with mice with different loxP site-flanked genes of interest, especially for time dependent gene expression [26]. Tamoxifen (Sigma-Aldrich) was dissolved in corn oil at a concentration of 10 mg/ml. 100 μ l dissolved tamoxifen solution was used via intraperitoneal injection once a day for a total of five consecutive days. And the mice waited for one week before the starting of experiments after the final injection. The mice were stimulated with LPS 10 mg/kg for 12 h and then sacrificed (Fig. 1A).

In order to find out the function of HIF-1 α /HO-1 signaling pathway in Golgi stress in vivo, the C57BL/6 mice were treated with DMOG (25 mg/ml, 300 μ l) by i. p. injection. And DMOG were dissolved in DMSO. The mice were randomly divided into four groups: ctrl group, LPS group, LPS + DMOG group, LPS + DMSO group (n = 6) for each group. After the treatment of DMOG for 24 h, the mice were stimulated with LPS 10 mg/kg for 12 h before sacrificing. All the procedures were performed according to National Institutes of Health guidelines. The mice were fed with standard laboratory diet and water at 25 $^{\circ}$ C, and lived in the animal room with 12 h light-dark cycle (Fig. 1C).

2.3. Terminal deoxynucleotidyl transferase (TdT) dUTP nick-end labeling (TUNEL) assay

TUNEL assay was performed to detect the apoptotic cells in lung tissue. The staining was processed according to the instruction of DeadEnd™ Fluorometric TUNEL System kit (Promega, Madison, WI, USA). Lung tissue slides were deparaffinated first and then incubated with proteinase K solution (20 μ g/ml in PBS) for 8–10 min. TUNEL labeling buffer (a mix of 45 μ l equilibration buffer, 5 μ l nucleotide mix, and 1 μ l recombinant terminal deoxynucleotidyl transferase (rTdT) enzyme) was added and incubated them in a humidified and lucifugal box for 1 h at 37 $^{\circ}$ [25]. Protect the slides from light until the end of the experiment. The cell nucleus was stained with DAPI fluorescent dye (Roche Life Science, United States) for 10 min. The images were taken by a fluorescence microscope (Olympus, Tokyo, Japan) after mounting with antifade solution.

2.4. Cell differential in bronchoalveolar lavage fluid (BALF), ELISA and histology

Mice were euthanized after 12 h of LPS injection, and the lungs were lavaged with PBS (0.5 ml each time, three times in total). Total leukocytes number in the BALF were counted by hemocytometer. Cellular differential results were performed by BALF and stained with Hema 3 (Fisher Scientific, #274297). The left lung was used for histology, and the right lung was used for qPCR and Western blot. Albumin and interleukin 6(IL-6) concentrations in the BALF were measured by ELISA kit according to the protocol (DuoSet, R&D Systems, Minneapolis, MN, USA).

2.5. Hematoxylin and eosin staining (HE staining)

The left lung tissues were fixed in 10% formaldehyde, embedded in

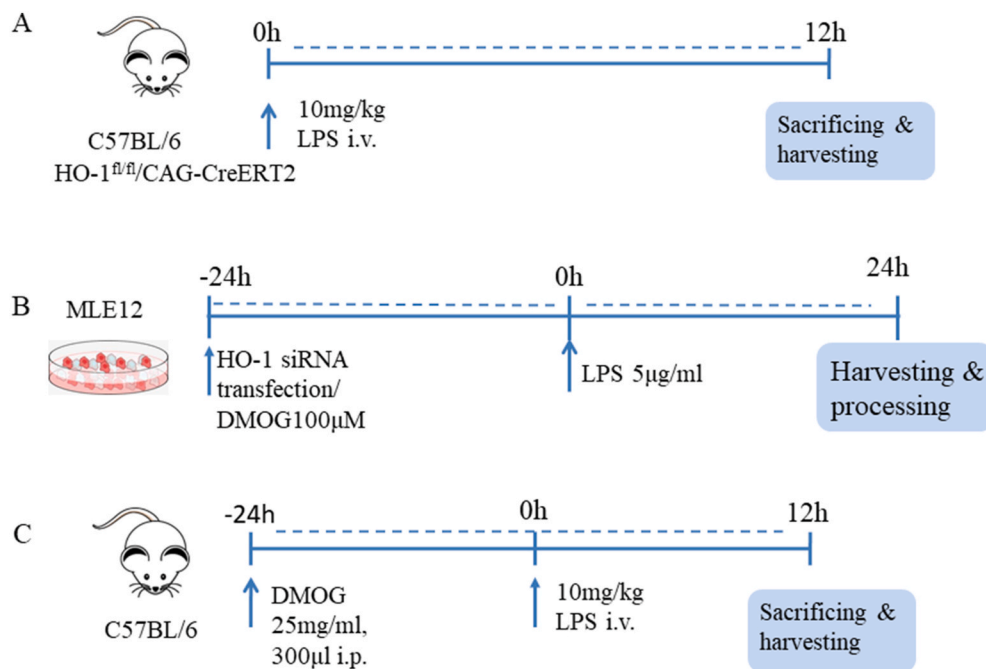


Fig. 1. Schematic diagram of the experimental methods in this research. **Fig. 1A.** C57BL/6 and HO-1^{fl/fl}/CAG-CreERT2 mice were injected with 10 mg/kg LPS through caudal vein, and euthanized for tissue collection after 12 h. **Fig. 1B.** MLE12 cells were transfected with HO-1siRNA for 24 h and then incubated with 5 µg/ml LPS for another 24 h before harvesting. To explore the function of HIF-1α/HO-1 pathway in Golgi stress in vitro, MLE12 cells firstly were pre-treated with 100 µM DMOG (dissolved in DMSO) for 24 h before 5 µg/ml LPS incubation for another 24 h. **Fig. 1C.** In order to find out the role of HIF-1α/HO-1 pathway in Golgi stress in vivo, C57BL/6 mice were pretreated with DMOG 25 mg/ml, 300 µl by intraperitoneal injection for 24 h, and then stimulated with LPS for 12 h before sacrificing.

paraffin, sectioned at 5 µm thick and stained with hematoxylin and eosin (H&E). H&E-stained slides were observed with a light microscope (Olympus, Nagano, Japan) after dehydration and sealing.

2.6. Measurement of intracellular reactive oxygen species (ROS) production

ROS levels were measured by dichloro-dihydro-fluorescein diacetate (DCFH-DA) probe (Beyotime Institute of Biotechnology, Nanjing, China). The cells were seeded in 96-well plates and cultured to 90% confluence. DCFH-DA was diluted to 10 µM with serum free medium. Then the cell suspension was loaded with DCFH-DA for 30 min at 37 °C, and mixed them every 3–5 min interval. Last the cells were washed in serum free medium for 3 times. DCF fluorescence was calculated with excitation and emission wavelengths of 485 and 535 nm. The differences relative to the initial fluorescence were analyzed in the results.

2.7. Cell culture

MLE12 cells were cultured in HITES medium supplemented with 2% fetal bovine serum, which is formulated at the ATCC as follows: Dulbecco's medium: Ham's F12, 50:50 mix; insulin 0.005 mg/ml; transferrin 0.01 mg/ml; sodium selenite 30 nM; hydrocortisone 10 nM, β-estradiol 10 nM; HEPES 10 mM; L-glutamine 2 mM; Fetal bovine serum 2%. A humidified atmosphere of 5% CO₂ and 95% air at 37 °C was provided for cell culture. The culture medium was changed every 3 days. In order to investigate the role of HO-1 in LPS-stimulated macrophages. The cells were cultured into 12 and 6 well plates. These cells were randomly divided into four groups: control group, LPS group (5 µg/ml), control siRNA + LPS (5 µg/ml), HO-1 siRNA + LPS (5 µg/ml). Control siRNA and HO-1 siRNA were used for transfection (50pM for 24 h) mixed with Lipofectamine RNAiMAX reagent (Invitrogen, Carlsbad, CA, USA) in OPTI-MEM media (Gibco, Carlsbad, CA, USA) [27]. The cells were treated with LPS (5 µg/ml) for 24 h following the transfection for 24 h, and then were harvested for further research. To find the function of HIF-1α/HO-1 signaling pathway, the prolyl hydroxylase inhibitor dimethylxalylglycine (DMOG, Millipore Sigma, D3695) was used to induce the stabilization of HIF-1α, as well as HO-1. MLE12 cells were divided into four groups: control group, LPS group, LPS + DMOG group,

LPS + DMSO group. MLE12 cells were pretreated with 100 µM DMOG (dissolved in DMSO) for 24 h, then stimulated with 5 µg/ml LPS for another 24 h before harvesting (Fig. 1B).

2.8. Real-time reverse transcriptase-polymerase chain reaction (RT-PCR)

Total RNA in tissue and cells was isolated by using Trizol (Invitrogen Life Technologies, Carlsbad, CA). Then cDNA was created using reverse transcriptase (Thermos Fisher, EP0442). AceQ Universal SYBR qPCR Master Mix (Vazyme Biotech Co., Ltd) was used for real time PCR. Gene-specific primers used in this experiment were shown in Table 1. The total volume of PCR was 20 µl. The amplification process was as follows: 95 °C for 5 min, followed by 40 cycles of 95 °C for 10 s and 60 °C for 30 s. The quantification of target gene levels were calculated by $2^{-\Delta\Delta CT}$ method.

2.9. Immunofluorescence staining

The lung tissue slices and the cells were fixed with 4% paraformaldehyde for 10 min, and then washed with PBS for three times. After incubating the primary antibody overnight, the tissue and slides were incubated with fluorescein-conjugated secondary antibody for 1 h. Anti-GM130 antibody (610822; BD Bioscience) and DAPI were used for Golgi and nuclear structure, respectively. Fluorescence pictures were obtained with Nikon confocal fluorescence microscope.

2.10. Electron microscopy

Lung tissue and MLE12 cells were fixed in 1.5% glutaraldehyde for 2 h and then postfixed in 1% osmium tetroxide. The samples were dehydrated in ethanol and embedded in Epon resin. Ultrathin sections of 100 nm were cut with Leica Ultramicrotome UC7. Uranyl acetate and lead citrate were used to stain the sections. Last, sections were viewed by a transmission electron microscope (HT7700; Hitachi, Tokyo, Japan).

2.11. Western blot analysis

The proteins were extracted from right lung tissue using a total and nuclear protein isolation kit (Thermo Fischer Scientific, Inc.). After the cells were treated with LPS(5ug/ml) for 24 h, cells were washed with

Table 1
Primers for detection of mRNA transcripts.

| genes | Forward primer | Reverse primer | Length (bp) |
|----------------|--------------------------|------------------------|-------------|
| GM130 | ATCTTGCCAGCCGTCTACAG | TGCCTCAGGTGCTCATTACITT | 178 |
| Mannosidase II | GTCACCTGGACTACCTCGG | CGTAGCAAAGCGTCCAAAT | 104 |
| Golgin97 | AAGGACTGGCTTTGGCATT | CATGTGCTTCACTTTGCTGATT | 197 |
| GOLPH3 | AAGGTTACAGTTAGAGGCTTGTGG | CCTGTTGGAGCATCCGATTTA | 84 |
| HO-1 | GAATCGAGCAGAACCAGCCT | CTCAGCATTCTCGGCTTGG | 135 |
| β -actin | CGTTGACATCCGTAAGACCTC | TAGGAGCCAGGGCAGTAATCT | 110 |

phosphate-buffered saline and then homogenized in RIPA buffer (Beyotime, P0013B). The concentrations of these proteins were detected using a BCA protein assay kit (Thermo, USA). Equal amounts of protein were subjected to 10% SDS-PAGE gel and then were transferred to a PVDF membrane (Millipore Cat #IPVH00010). Membranes were blocked with 5% nonfat powdered milk in TBST (PBS with 0.05% Tween 20) for 1 h and incubated overnight at 4 °C with primary antibody against β -actin (1:8000 dilution, Tianjin Sanjian, #KM9001), HO-1 (1:1000 dilution, PTG, #10701), GM-130 (1:200 dilution, Santa, #55590), mannosidase II (1:200 dilution, Santa, #376909), Golgin97 (1:1000 dilution, CST, #13192), GOLPH3 (1:1000 dilution, PTG, #19112). Next, the blots were washed by TBST for 3 times (10 min for each time). After washing, the horseradish peroxidase-conjugated goat anti mouse immunoglobulin G (1:10,000 dilution, Tianjin Sungene Biotech Co., Ltd, Cat #LK2003). The blots were visualized by enhanced chemiluminescence and quantified by densitometry (Molecular Analysis Image-analysis Software, Bio-Rad, USA).

2.12. Statistical analysis

The values are expressed as mean \pm standard deviation (SD). T-test

and nonparametric tests were used for comparisons between two groups. One-way ANOVA was used to make comparisons among multiple groups, followed by the Bonferroni correction post hoc test. Graph Prism 7.0 software (GraphPad Software, USA) was used for statistical analysis. Statistical significance was considered at $P < 0.05$.

3. Results

3.1. The stimulation of LPS induced acute lung injury and Golgi stress in wild type mice

C57BL/6J mice were exposed to LPS (10 mg/kg) or PBS (control) for 12 h and the BALF was obtained for cell differential and ELISA. HE staining was used to evaluate the pathological changes in our study. These slices showed that LPS induced the thickening of alveolar septum, inflammatory cells accumulation, hemorrhage and hyaline membrane formation (Fig. 2A). IL-6 and albumin contents in BALF and ROS in lung tissue were higher after the treatment of LPS (Fig. 2B–D). LPS significantly increased the total leukocytes number, as well as lymphocytes, neutrophils number in BALF when compared with the control group (Fig. 2E & supplementary data Fig. 1A–C). TUNEL staining was used to

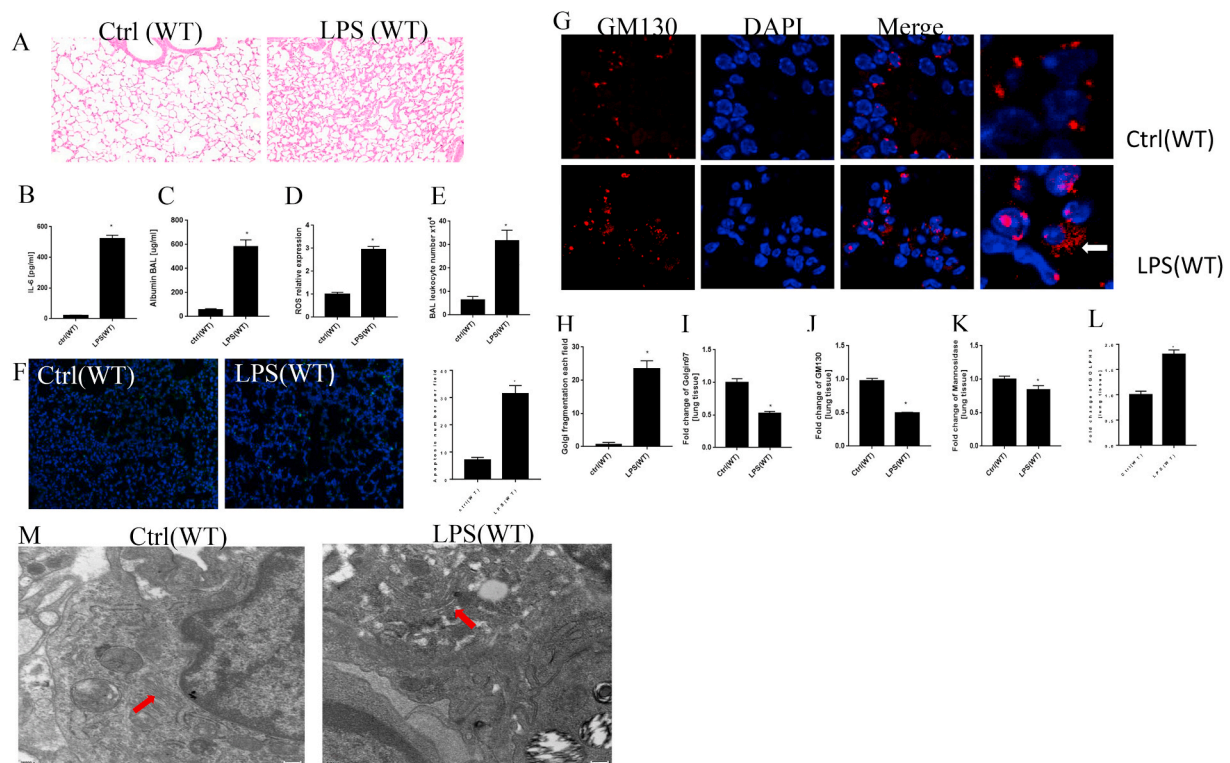


Fig. 2. LPS enhanced oxidative stress and Golgi stress along with acute lung injury in mice. HE staining for lung tissue in WT mice after the treatment of 10 mg/kg LPS and PBS for 12 h (Fig. 2A). Albumin and IL-6 were detected in BALF by ELISA (Fig. 2B and C). ROS levels in lung tissue (Fig. 2D). Total leukocytes number in BALF (Fig. 2E). TUNEL staining for apoptosis in lung tissue (Fig. 2F). Golgi structure changes in confocal (Fig. 2G and H). mRNA levels of Golgi morphology related proteins and GOLPH3 (Fig. 2I–L). Golgi structure changes in electron microscope (Fig. 2M). * $P < 0.05$ vs. control, $N = 3$ at least for each group. Data were presented as mean \pm SD, and were analyzed by *t*-test.

see the apoptosis levels of lung tissue after the injection of LPS (Fig. 2F). TUNEL positive cell numbers were significantly higher in LPS group than that in control group (Fig. 2F). Therefore, we concluded that LPS induced oxidative stress, inflammation, apoptosis along with acute lung injury in WT mice.

GM130, localized on the cis side of the Golgi cisternae, is involved in the disassembly and reassembly of the Golgi during the process of mitosis, thus it regarded as a specific marker for the Golgi apparatus [28]. Golgin97, which is located in the trans-Golgi network, plays crucial roles in vesicle trafficking and maintaining the Golgi integrity [29]. Mannosidase II is related to oligosaccharide processing in N-linked glycoprotein biosynthesis and regarded as a marker for medial-Golgi compartments [30]. It has been found that GOLPH3 is one of Golgi stress inducible proteins in oxygen-glucose deprivation and reoxygenation treated N2A cells [31]. Further studies on the morphology changes of Golgi was performed using the double immunofluorescence (IF) with FITC-labeled GM130-antibody (red) and DAPI(blue, nuclear staining). As shown in Fig. 2G, Golgi apparatus localized to a compact perinuclear ribbon in control group. Meanwhile, some of the red staining diffused into the cytoplasm and the structures of Golgi fragmented into a lot of punctate structures with high intensity in the cytoplasm in LPS treatment group (Fig. 2G). Thus, LPS treatment induced GA stress response in mice. Furtherly, the Golgi fragmentation percentage was much higher in LPS group (Fig. 2H). Fig. 2I-L showed that LPS downregulated the mRNA expression of GM130, Golgin97, mannosidase II, and increased the levels of GOLPH3. In order to further characterize the morphology of Golgi in lung tissue, electron microscopy (EM) analyses were performed. Figure 2M showed that the control lung tissue had typical long Golgi ribbon structures near the nucleus. And LPS treatment induced the swelling of GA structure and more mini-stacks.

3.2. HO-1 knockout accelerated lung injury and Golgi fragmentation in endotoxin-induced acute lung injury

HO-1 is one of inducible proteins in many diseases under the insults of oxidative stress and inflammatory response [32]. It has been demonstrated that the protective effect of HO-1 is related to maintaining the homeostasis of organelles in cells, such as mitochondria, endoplasmic reticulum and so on [14,15]. In this research, we try to find out the effect of HO-1 on Golgi stress in endotoxin-induced acute lung injury. HO-1^{fl/fl}/CAG-CreERT2 and CAG-CreERT2 mice were used to explore the function of HO-1 on Golgi stress after the treatment of LPS (10 mg/kg) for 12 h.

CRISPR-cas9 strategy was used to generated Hmox1^{fl/fl} (HO-1^{fl/fl}) mice and selectively knockout exon2-3 in the C57/B6 background (Fig. 3A). Sequencing and southern blotting were used to verify the insertion of the loxp site. HO-1^{fl/fl} mice were crossed with CAG-iCreERT2 mice (C57BL/6 background) to obtain HO-1^{fl/fl}/CAG-CreERT2 homozygote mice. The mice were sacrificed for further research after the administration of LPS(10 mg/kg) for 12 h through caudal vein injection.

HE staining from Fig. 3B showed that the knockout of HO-1 exaggerated lung injury. Albumin and IL-6 in BALF were higher in HO-1 knockout mice, when compared with LPS(Cre) group (Fig. 3C and D). ROS levels in lung tissue also increased after the knockout of HO-1 (Fig. 3E). Total leukocytes number in BALF increased significantly in HO-1KO group after the treatment of LPS (Fig. 3F). Cell differential results from BALF showed that the knockout of HO-1 increased the number of macrophages and neutrophils number in BALF (supplemental data Fig. 1D–F). More apoptosis cells were found after the knockout of HO-1 in lung tissue (Fig. 3G). Further studies on Golgi structure were performed by immunofluorescence (Fig. 3H). There were more Golgi fragmented into a lot of punctate structures in the cytoplasm in HO-1KO group (Fig. 3H and I). Fig. 3J-L showed that mRNA levels of Golgin97, GM130, mannosidase II decreased after the knockout of HO-1. To the

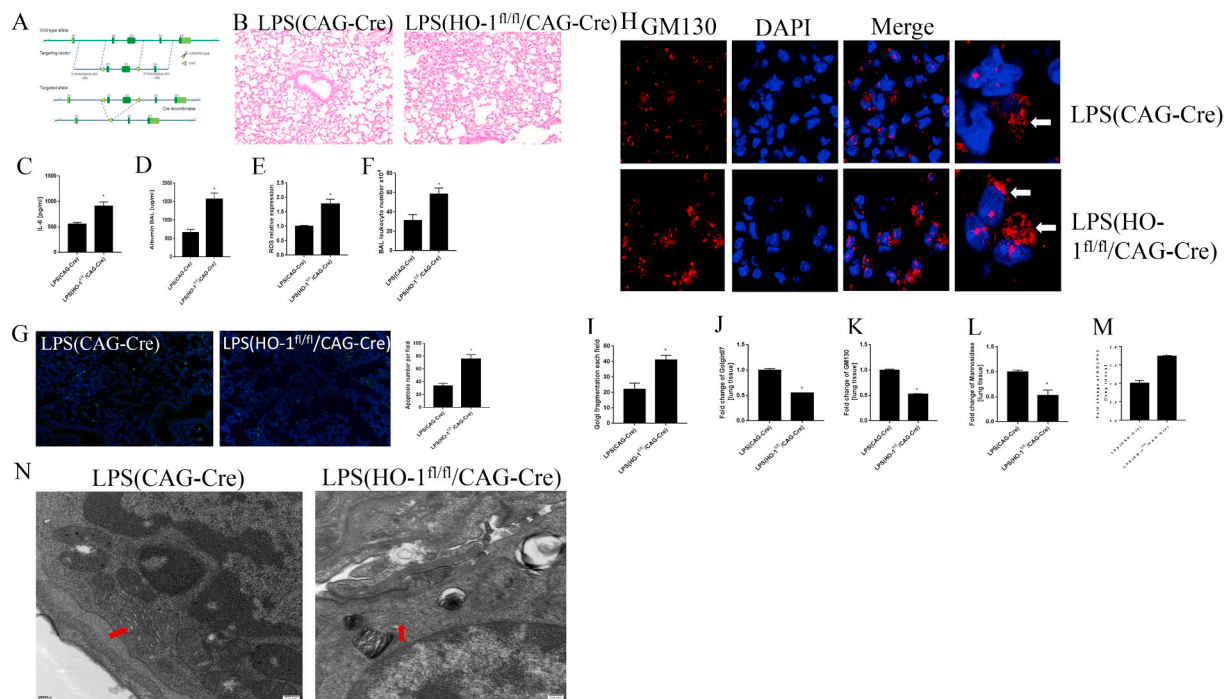


Fig. 3. HO-1 deletion exaggerated oxidative stress and Golgi fragmentation after the treatment of LPS in vivo. Fig. 3A CRISPR/Cas9 technology was used to generate HO-1 knockout mice. HE staining for lung tissue (Fig. 3B). Albumin and IL-6 levels in BAL and ROS in lung tissue (Fig. 3C–E). Total leukocytes number in BALF (Fig. 3F). TUNEL staining for apoptosis in lung tissue (Fig. 3G). Immunofluorescence staining to see Golgi morphology changes in lung tissue (Fig. 3H and I). qPCR results showed the mRNA expression levels of Golgi morphology related proteins and GOLPH3 in vivo (Fig. 3J–M). Golgi structure changes in electron microscope (Fig. 3N). *P < 0.05 vs. control, N = 3 at least for each group. Data were presented as mean ± SD, and were analyzed by t-test.

contrary, the mRNA expression levels of GOLPH3 increased, which furtherly demonstrated the exaggerated Golgi stress in HO-1 knockout mice after the stimulation of LPS (Fig. 3M). The electron micrographs revealed that the Golgi apparatus was turned to small stacks with similar number of cisternae after the knockout of HO-1 when compared with that in CAG-Cre mice (Fig. 3N). These results indicated that HO-1 knockout causes the fragmentation of Golgi apparatus.

3.3. The knockdown of HO-1 exacerbate oxidative stress and Golgi fragmentation in MLE12 cells

Alveolar epithelial cells play an important role in lung development and repair in acute lung injury because of their self-renewal capacity and immunomodulatory function [33]. Therefore, we used epithelial cells to explore the function of HO-1 on Golgi stress in vitro. To see the oxidative stress levels after the incubation of LPS, cell viability, ROS contents, SOD activity were analyzed. To simulate the cell model of ALI, MLE12 cells were incubated with different concentrations of LPS, then the cell viability was assessed after 24 h. Fig. 4A showed the cell viability significantly decreased, when LPS concentration increased to 1 $\mu\text{g/ml}$, 5 $\mu\text{g/ml}$, 10 $\mu\text{g/ml}$. Cell viability was inhibited after the treatment of LPS 5 $\mu\text{g/ml}$, especially in LPS + HO-1siRNA group (Fig. 4B). Therefore, we used 5 $\mu\text{g/ml}$ as our LPS treatment concentration in vitro. Compared to the control group, LPS significantly increased the expression levels of ROS and decreased the activity of SOD. Furtherly, LPS + HO-1 siRNA group had higher expression levels of ROS and lower activity of SOD when compared with LPS and LPS + NC group (Fig. 4C and D). To gain

sight into the structure change of Golgi, the MLE12 cells were stained with immunofluorescence. As shown in Fig. 4E, the number of Golgi fragmentation was increased after LPS insult. Lots of ribbon-like GA near nuclei turned to debris-like structures which were scattered in the cytoplasm after 24 h treatment with LPS. And the knockdown of HO-1 furtherly increased the Golgi fragmentation. The structure of Golgi was also evaluated by electron microscope. From Fig. 4F, we know that cisternal membrane of GA was closely stacked and highly ordered. In contrast, LPS stimulation induced dilated, and less well organized GA cisterna. Furtherly, the cisterna of GA tended to be fragmented and mini-stacks after the knockdown of HO-1 in LPS-stimulated MLE12 cells.

3.4. HO-1 deletion reduced the expression levels of Golgi morphology related proteins and induced the expression of Golgi stress related protein in LPS stimulated MLE12 cells

In order to see the expression levels of Golgi morphology related proteins, western blots were used to detect the protein levels. The results showed that protein levels of GM130, Golgin 97 and mannosidase II reduced significantly in LPS treated groups, and the knock down of HO-1 by siRNA furtherly inhibited the expression of these proteins (Fig. 5A–E). To the contrary, the protein levels of HO-1 and GOLPH3 increased obviously after the stimulation of LPS. GOLPH3 levels were furtherly increased after the knockout of HO-1 in MLE12 cells (Fig. 5A, B, F). Data from these experiments suggested that the fragmentation of Golgi were related to the changes of these proteins.

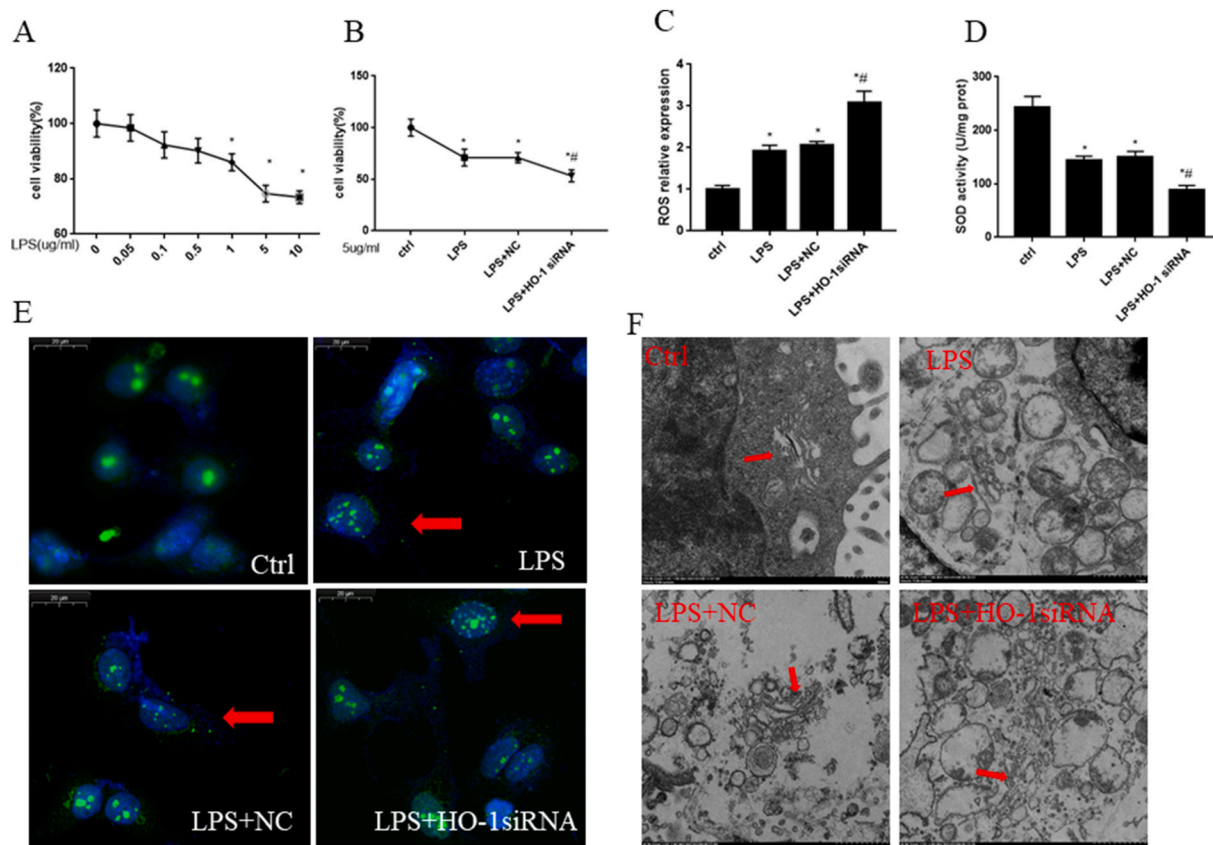


Fig. 4. The knock down of HO-1 exacerbated oxidative stress and Golgi fragmentation in MLE12 cells. Cell viability significantly decreased when the cells were incubated with LPS for 24 h at the concentration of 1 $\mu\text{g/ml}$, 5 $\mu\text{g/ml}$ and 10 $\mu\text{g/ml}$ (Fig. 4A). HO-1 siRNA transfection (50pM for 24 h) were used to knockdown the expression of HO-1 and then the cells were incubated with 5 $\mu\text{g/ml}$ LPS for another 24 h. The cell viability was reduced after the treatment of LPS when compared with the control group. Furtherly HO-1 knockdown group showed much lower cell viability (Fig. 4B). ROS and SOD activity in MLE12 cells (Fig. 4C–D). Fluorescent staining results show Golgi morphology changes and Golgi fragmentation numbers for each field in vitro (Fig. 4E). Golgi structure changes were evaluated by electron microscope (Fig. 4F). * $P < 0.05$ vs. control, # $P < 0.05$ vs. LPS group. $N = 3$ at least for each group. Data were presented as mean \pm SD, and were analyzed by one-way analysis of variance (ANOVA), followed by the Bonferroni correction post hoc test.

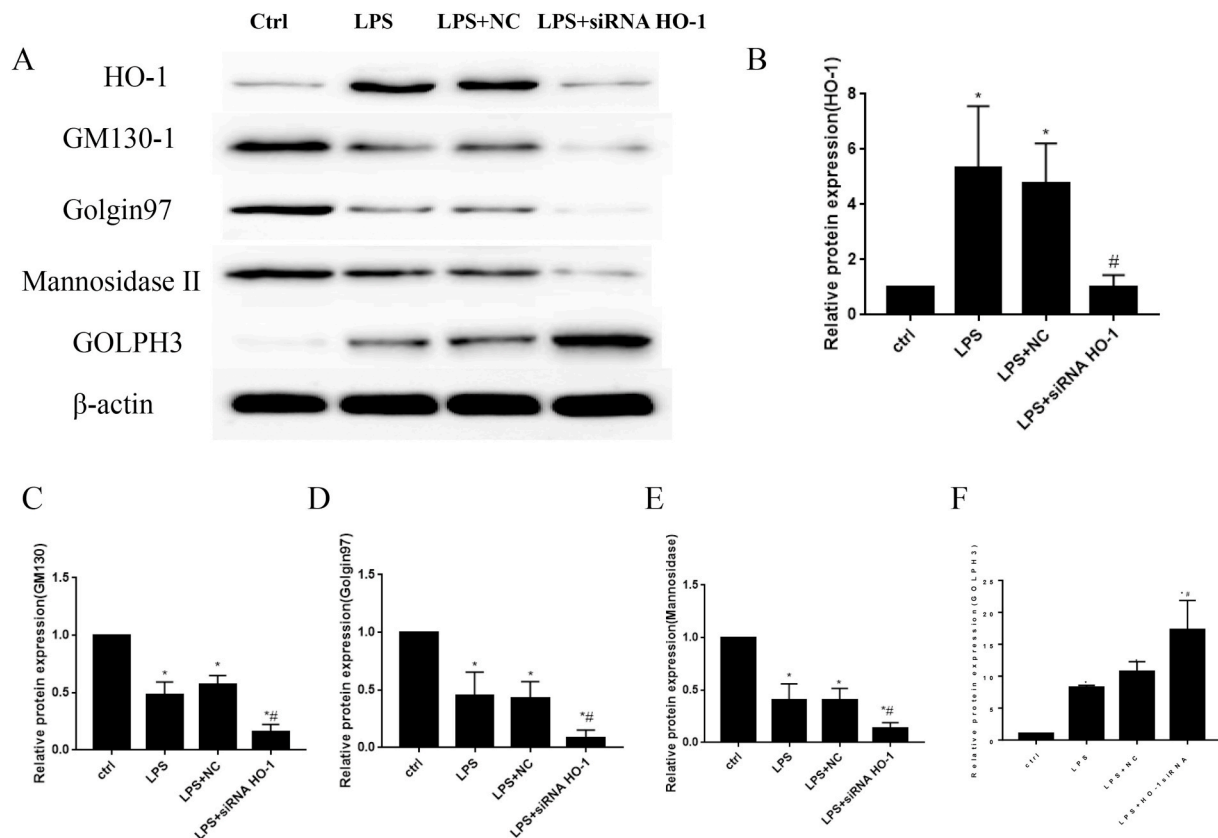


Fig. 5. HO-1 knockdown decreased Golgi morphology related proteins expression and increased Golgi stress related protein expression in vitro. Protein levels of HO-1, GM130, Golgin97, mannosidase II and GOLPH3 in MLE12 cells (Fig. 5A–F). *P < 0.05 vs. control, #P < 0.05 vs. LPS group. N = 3 at least for each group. Data were presented as mean \pm SD, and were analyzed by one-way analysis of variance (ANOVA), followed by the Bonferroni correction post hoc test.

3.5. The activation of HIF-1 α /HO-1 signaling pathway prevent Golgi stress and fragmentation in vivo

Hypoxia-inducible factor (HIF)-1 α is a transcription factor which is involved in the regulation of lots of genes no matter in physiological or pathological conditions [34]. Under normoxia conditions, the activity of HIF-1 α subunit is negatively regulated by prolyl hydroxylase (PHD), which hydroxylates proline residues and induce its degradation through proteasome pathways [35]. DMOG is a kind of competitive inhibitor of the PHDs and has been proved to stabilize HIF-1 α in vivo and in vitro [36,37]. In order to verify the role of HIF-1 α /HO-1 signaling pathway on Golgi stress, we used DMOG to stimulate HIF-1 α /HO-1 signaling pathway and observed lung injury levels and Golgi structure and stress related proteins expression levels in vivo. The results showed that the lung tissue had reduced lung injury level after the treatment of DMOG (Fig. 6A). At the same time, the treatment of DMOG increased the protein levels of HIF-1 α , HO-1, Golgi structure proteins GM130, Golgin97 and mannosidase II, and decreased the expression of Golgi stress protein GOLPH3 in lung tissue of mice (Fig. 6B–H). Therefore, the activation of HIF-1 α /HO-1 signaling pathway attenuated acute lung injury and reduced Golgi stress by increasing the expression of Golgi structure proteins and decreased Golgi stress protein in vivo.

3.6. The activation of HIF-1 α /HO-1 signaling pathway prevent Golgi stress and fragmentation in vitro

In this research, we treated MLE12 cells with 100 μ M DMOG for 24 h before the treatment of 5 μ g/ml LPS for another 24 h to activate the expression of HIF-1 α /HO-1 signaling pathway. The results showed that LPS inhibited cell viability and SOD activity and enhanced the expression of ROS levels (Fig. 7A–C). To the contrary, the treatment of DMOG

improved cell viability, as well as SOD activity, and decreased the expression of ROS in vitro (Fig. 7A–C). Oxidative stress is caused by the imbalance of oxidative-antioxidative systems and along with increased free radical generation and reduced antioxidants activity [38]. It has been widely demonstrated that antioxidative enzyme activities decreased and free radical contents increased after the stimulation of various stress [39,40]. Superoxide dismutases (SOD) are a kind of antioxidant enzyme that catalyze the superoxide radicals ($O_2^{\cdot-}$) to molecular oxygen (O_2) and hydrogen peroxide (H_2O_2) [41]. Therefore, SOD activity decreased after the stimulation of LPS in vitro. And HO-1 is involved in cellular protection by decreasing oxidative stress, reducing cellular apoptosis and inflammatory response. The cells showed more oxidative stress levels after the knockdown of HO-1, which contributed to the attenuation of SOD activity [12,42].

In order to figure out the relationship between HIF-1 α /HO-1 signaling pathway and Golgi stress, Western blot was used to detect Golgi morphology and stress related proteins. And the results showed that DMOG significantly increased the protein expression levels of HIF-1 α and HO-1, as well as GM130, Golgin97 and mannosidase II expressions in LPS + DMOG group compared with LPS group. At the same time, the expression levels of GOLPH3 significantly reduced along with the activation of HIF-1 α /HO-1 signaling pathway. And there were no significant difference between LPS and LPS + DMSO group for these proteins (Fig. 7D–J).

4. Discussion

Golgi apparatus dysfunction has been increasingly regarded as one crucial factor to the pathogenesis of human disease [31,43]. Our research provide strong evidence that LPS induced Golgi morphology fragmentation both in vivo and in vitro. HO-1 knockdown increased the

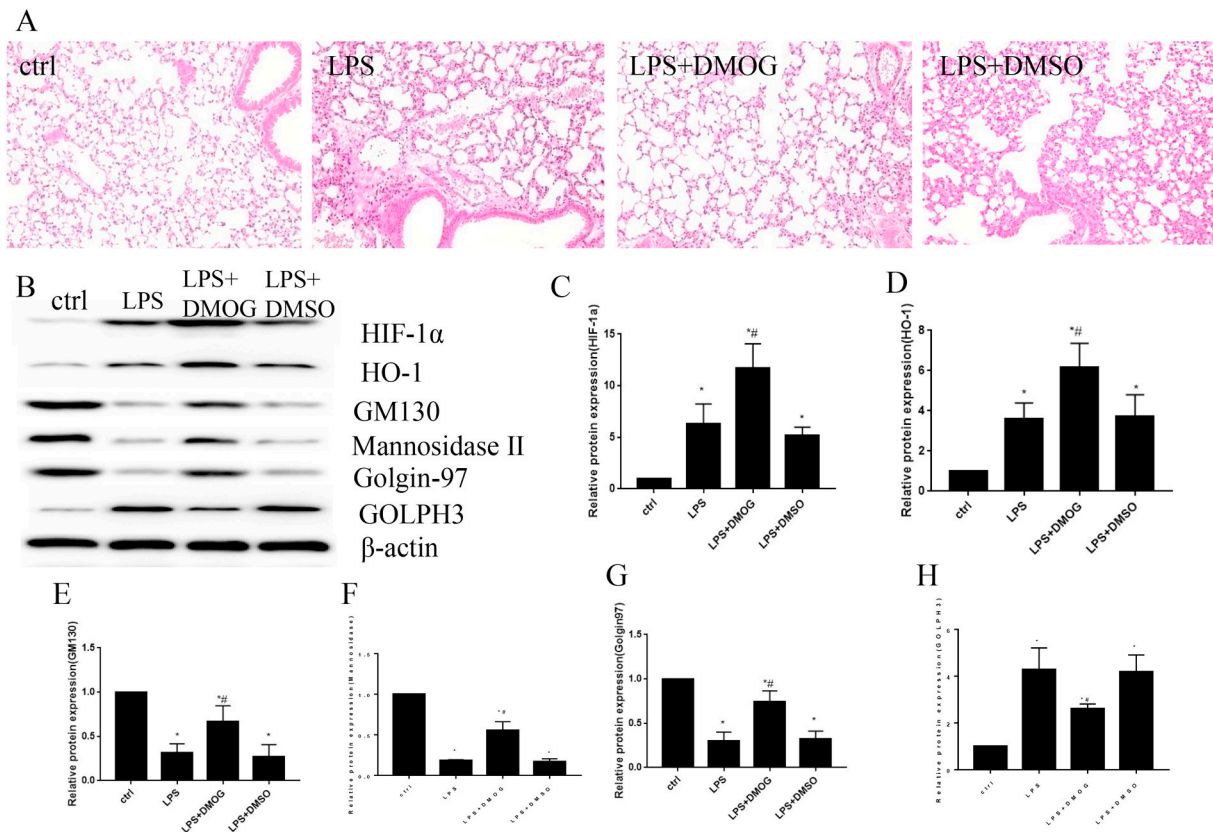


Fig. 6. The activation of HIF-1 α /HO-1 signaling pathway improved Golgi stress in vivo. The C57BL/6 mice were pretreated with DMOG to activate HIF-1 α /HO-1 signaling pathway and then treated with LPS to induce acute lung injury. The lung tissue injury levels by HE staining (Fig. 6A). The Western blot to show the protein levels of HIF-1 α , HO-1, GM130, mannosidase II, Golgin97 and GOLPH3 in lung tissue (Fig. 6B–H). *P < 0.05 vs. control, #P < 0.05 vs. LPS group. N = 3 at least for each group. Data were presented as mean \pm SD, and were analyzed by one-way analysis of variance (ANOVA), followed by the Bonferroni correction post hoc test.*.

expression of ROS, Albumin, IL-6, enhanced cell apoptosis and leukocytes accumulation in vivo. Further, HO-1 protect acute lung injury via increasing the expression of Golgi morphology proteins, such as GM130, mannosidase II, Golgin 97, and inhibit the expression of Golgi stress protein GOLPH3 in vivo and in vitro. And the activation of HIF-1 α /HO-1 signaling pathway prevent Golgi fragmentation by increasing the expression of GM130, mannosidase II, Golgin97, and decreasing the expression of GOLPH3.

The Golgi apparatus is the center of the secretory pathway and precisely regulates various functions, such as the modification, sorting and delivery of some secretory cargoes [44]. Golgi dispersal may be a kind of compromise response for cellular stress resistance, because its membranes will lose some antioxidant molecules and some factors crucial for redox homeostasis, which could propagate Golgi-derived lipid peroxides [45]. Under some toxic conditions, Golgi membranes can produce some lethal lipid ROS species, which could be transported to other compartments [45]. Recently, more and more research have found that oxidative stress can also affect the structure and normal physiological function of the GA [1,5,46]. ROS can not only impair Golgi-associated vesicular trafficking and protein sorting processes, but also influence glycosylation [47]. Further, the changes of GA may trigger some downstream stress signals or even promote apoptosis. Many apoptotic regulatory components, such as proapoptotic caspase-2, Fas, tumor necrosis factor receptor-1, Bcl-2 family members, are located in GA and the activation of these apoptotic factors reversely induce Golgi structure and trafficking proteins cleavage such as golgin-160 [48], GM130 [49], giantin [50], GRASP65 [51] and so on. In this research we observed the fragmentation of Golgi and the disruption of Golgi morphology related protein expression levels in septic-induced lung injury in vivo and in vitro. Our results indicated that LPS

decreased the levels of GM130, mannosidase II (medial-Golgi marker) and Golgin97 (trans-Golgi marker), which were furtherly decreased after the knockdown of HO-1. Reversely, the activation of HIF-1 α /HO-1 increased the expression of GM130, mannosidase II and Golgin 97 and protect the Golgi from oxidative stress injury.

Some neurodegenerative disease, such as Alzheimer's and Parkinson's are also related to Golgi fragmentation, oxidative stress and lipid peroxide generation [52,53]. For example, the loss of GM 130 leads to the impairment of secretory trafficking and the disruption of Golgi architecture and function in neurodegenerative disease [54]. However, the mechanism of Golgi stress in the development of some lung diseases remain poorly understood. Weidner J et al. reported that there were disruption among endoplasmic reticulum (ER), Golgi, and lysosomes in fibroblasts from COPD patients [55]. And they found the size of Golgi decreased in COPD patients, but the reason for this change is still not so clear [55]. GOLPH3(also named GMx33 and GPP34), a peripheral membrane protein, is localized to the trans-Golgi and extract vesicles from the Golgi [56]. Li T et al. found that the expression levels of GOLPH3 significantly increased in oxygen-glucose deprivation and reoxygenation treated N2A cells [31]. Further, the elevated expression of GOLPH3 stimulated the ROS production and stress-related autophagy [31]. Yu KN et al. found cigarette smoke condensate treatment could increase ROS generation and disrupt endoplasmic reticulum-Golgi network homeostasis via GOLPH3 overexpression and abnormal autophagy in lung epithelial cells [57]. In this research, the expression levels of GOLPH3 increased after the treatment of LPS, especially after the knockout of HO-1 both in vivo and in vitro. To the contrary, the activation of HIF-1 α /HO-1 signaling pathway inhibited the expression of GOLPH3, along with the reduced oxidative stress response.

Septic-induced acute lung injury can rapidly result in the

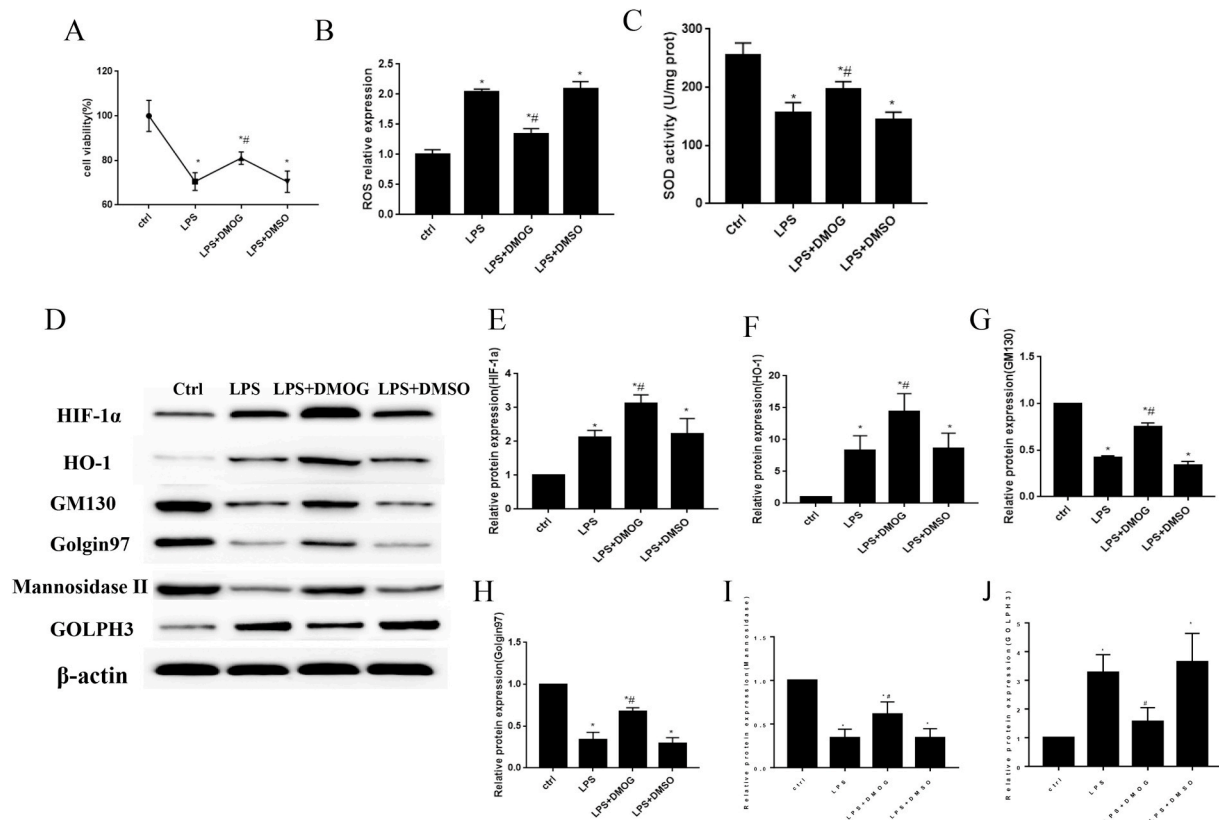


Fig. 7. The activation of HIF-1 α /HO-1 signaling pathway improved Golgi stress in vitro. The MLE12 cells were pretreated with 100 μ M DMOG for 24 h and then incubated with LPS for another 24 h to increase the expression of HIF-1 α and HO-1 in MLE12 cells. The results showed that DMOG treatment increased cell viability (Fig. 7A) and SOD activity (Fig. 7C) and decreased ROS expression (Fig. 7B) when compared with LPS group. The Western blot was used to measure the protein levels of HIF-1 α , HO-1, GM130, mannosidaseII, Golgin97 and GOLPH3 in vitro (Fig. 7D–J). * $P < 0.05$ vs. control, # $P < 0.05$ vs. LPS group. $N = 3$ at least for each group. Data were presented as mean \pm SD, and were analyzed by one-way analysis of variance (ANOVA), followed by the Bonferroni correction post hoc test.*.

development of pulmonary inflammation, the alveolar-capillary membrane damage and the acute respiratory distress syndrome (ARDS) [58]. Many studies have demonstrated that oxidative stress is involved in the pathogenesis and progression of acute lung injury and sepsis [12,59,60]. Additionally, it has been clarified that some organelles in cells, such as mitochondria and ER, are the crucial targets for oxidative damage during acute lung injury [12,61]. Our previous research have demonstrated that heme oxygenase-1 could diminish oxidative stress injury by regulating mitochondrial morphology in LPS-induced acute lung injury in vivo and in vitro [12,62]. In this research, we found that the deletion of HO-1 could aggravate Golgi fragmentation and Golgi stress through reducing the expression of GM130, mannosidaseII, Golgin 97, enhancing the levels of GOLPH3 and deteriorating oxidative stress levels in LPS-induced acute lung injury both in vivo and in vitro.

The Golgi apparatus is one of the most complicated organelles in the cells. More and more researches are focused on the morphology and function changes of Golgi in some oxidative stress related diseases [1,5,6]. However, the molecular mechanisms and its relative physiological functions of the Golgi stress has not been clarified. The interplay among different organelles, such as ER, Golgi, mitochondria, is intricate and finding their communication among them would also be of great importance. Therefore, it would be of great interest to find out more elaborate regulations in this aspect, which will provide some new understanding and therapy methods for more diseases in future.

5. Conclusions

Golgi stress is involved in the progression of endotoxin-induced acute lung injury both in vivo and in vitro. HO-1 protects against septic lung injury by inhibiting Golgi stress, increasing the expression of

Golgi structure related proteins, and reducing oxidative stress and inflammation. Furtherly, the protective effect of HO-1 on Golgi stress was enhanced by the activation of HIF-1 α /HO-1 signaling pathway. In conclusion, HO-1 plays a crucial role in alleviating sepsis-induced acute lung injury by regulating Golgi stress, and HIF-1 α /HO-1 signaling pathway is one of mechanisms for the regulation of Golgi stress, which may provide a therapeutic target for the treatment of acute lung injury.

Author contributions

XY Li, JB Yu, LR Gong designed the study, analyzed and interpreted data. Y Zhang, SA Dong, J Shi performed statistical analysis. C Li, YT Li, YF Zhang supervised the study. XY Li drafted the manuscript. JB Yu, LR Gong critically reviewed the manuscript. HB Li did some experiments for supplemental data. All the authors did final approval of the version to be submitted.

Funding statement

This work was supported by the grants from the National Natural Science Foundation of China (#81772106), China; the Youth Fund of the National Natural Science Foundation of China (#81601707), China; Key project of Tianjin Natural Science Foundation(18JJCZDJ35400), China.

Declaration of competing interest

The authors declare that no competing interests exist.

Appendix A. Supplementary data

Supplementary data to this article can be found online at <https://doi.org/10.1016/j.freeradbiomed.2021.01.028>.

References

- [1] S.W. Hicks, C.E. Machamer, Golgi structure in stress sensing and apoptosis, *Biochim. Biophys. Acta* 1744 (3) (2005) 406–414.
- [2] C. Ranftler, C. Meisslitzer-Ruppitsch, J. Neumuller, A. Ellinger, M. Pavelka, Golgi apparatus dis- and reorganizations studied with the aid of 2-deoxy-D-glucose and visualized by 3D-electron tomography, *Histochem. Cell Biol.* 147 (4) (2017) 415–438.
- [3] A.K. Gillingham, S. Munro, Finding the Golgi: golgin coiled-coil proteins show the way, *Trends Cell Biol.* 26 (6) (2016) 399–408.
- [4] S. Nakagomi, M.J. Barsoum, E. Bossy-Wetzel, C. Sutterlin, V. Malhotra, S.A. Lipton, A Golgi fragmentation pathway in neurodegeneration, *Neurobiol. Dis.* 29 (2) (2008) 221–231.
- [5] Z. Jiang, Z. Hu, L. Zeng, W. Lu, H. Zhang, T. Li, H. Xiao, The role of the Golgi apparatus in oxidative stress: is this organelle less significant than mitochondria? *Free Radic. Biol. Med.* 50 (8) (2011) 907–917.
- [6] J. Li, E. Ahat, Y. Wang, Golgi structure and function in Health, stress, and diseases, *Results Probl. Cell Differ.* 67 (2019) 441–485.
- [7] D.H. Zhao, Y.J. Wu, S.T. Liu, R.Y. Liu, Salvianolic acid B attenuates lipopolysaccharide-induced acute lung injury in rats through inhibition of apoptosis, oxidative stress and inflammation, *Experimental and therapeutic medicine* 14 (1) (2017) 759–764.
- [8] X.T. Huang, W. Liu, Y. Zhou, M. Sun, H.H. Yang, C.Y. Zhang, S.Y. Tang, Galectin-1 ameliorates lipopolysaccharide-induced acute lung injury via AMPK-Nrf2 pathway in mice, *Free Radic. Biol. Med.* 146 (2020) 222–233.
- [9] X. Cao, COVID-19: immunopathology and its implications for therapy, *Nat. Rev. Immunol.* (2020).
- [10] Z. Xu, L. Shi, Y. Wang, J. Zhang, L. Huang, C. Zhang, S. Liu, P. Zhao, H. Liu, L. Zhu, et al., Pathological findings of COVID-19 associated with acute respiratory distress syndrome, *Lancet Respir Med* 8 (4) (2020) 420–422.
- [11] X. Chen, Y. Wang, X. Xie, H. Chen, Q. Zhu, Z. Ge, H. Wei, J. Deng, Z. Xia, Q. Lian, Heme oxygenase-1 reduces sepsis-induced endoplasmic reticulum stress and acute lung injury, *Mediat. Inflamm.* 2018 (2018) 9413876.
- [12] J. Yu, J. Shi, D. Wang, S. Dong, Y. Zhang, M. Wang, L. Gong, Q. Fu, D. Liu, Heme oxygenase-1/carbon monoxide-regulated mitochondrial dynamic equilibrium contributes to the attenuation of endotoxin-induced acute lung injury in rats and in lipopolysaccharide-activated macrophages, *Anesthesiology* 125 (6) (2016) 1190–1201.
- [13] L.E. Otterbein, R. Foresti, R. Motterlini, Heme oxygenase-1 and carbon monoxide in the heart: the balancing act between danger signaling and pro-survival, *Circ. Res.* 118 (12) (2016) 1940–1959.
- [14] H.B. Suliman, J.E. Keenan, C.A. Piantadosi, Mitochondrial quality-control dysregulation in conditional HO-1(-/-) mice, *JCI Insight* 2 (3) (2017), e89676.
- [15] H. Maamoun, T. Benamer, G. Pintos, S. Munusamy, A. Agouni, Crosstalk between oxidative stress and endoplasmic reticulum (ER) stress in endothelial dysfunction and aberrant angiogenesis associated with diabetes: a focus on the protective roles of heme oxygenase (HO)-1, *Front. Physiol.* 10 (2019) 70.
- [16] J. Shi, J. Yu, Y. Zhang, L. Wu, S. Dong, S. Du, D. Ma, PI3K/Akt pathway-mediated HO-1 induction regulates mitochondrial quality control and attenuates endotoxin-induced acute lung injury, *Lab. Invest.* 99 (12) (2019) 1795–1809.
- [17] X. Li, Y. Zhang, J. Yu, R. Mu, L. Wu, J. Shi, L. Gong, D. Liu, Activation of protein kinase C- α /heme oxygenase-1 signaling pathway improves mitochondrial dynamics in lipopolysaccharide-activated NR8383 cells, *Exp Ther Med* 16 (2) (2018) 1529–1537.
- [18] J. Yu, Y. Wang, Z. Li, S. Dong, D. Wang, L. Gong, J. Shi, Y. Zhang, D. Liu, R. Mu, Effect of heme oxygenase-1 on mitofusin-1 protein in LPS-induced ALI/ARDS in rats, *Sci. Rep.* 6 (2016) 36530.
- [19] J. Mazumdar, V. Dondeti, M.C. Simon, Hypoxia-inducible factors in stem cells and cancer, *J. Cell Mol. Med.* 13 (11–12) (2009) 4319–4328.
- [20] I. Calvo-Asensio, E.T. Dillon, N.F. Lowndes, R. Ceredig, The transcription factor hif-1 enhances the radio-resistance of mouse MSCs, *Front. Physiol.* 9 (2018) 439.
- [21] A. Gorga, G. Rindone, M. Regueira, M.F. Riera, E.H. Pellizzari, S.B. Cigorraga, S. B. Meroni, M.N. Galardo, HIF involvement in the regulation of rat Sertoli cell proliferation by FSH, *Biochem. Biophys. Res. Commun.* 502 (4) (2018) 508–514.
- [22] S.A.D. Santos, D.R.J. Andrade, HIF-1 α and infectious diseases: a new frontier for the development of new therapies, *Rev. Inst. Med. Trop. Sao Paulo* 59 (2017) e92.
- [23] S. Chillappagari, S. Venkatesan, V. Garapati, P. Mahavadi, A. Munder, A. Seubert, G. Sarode, A. Guenther, B.T. Schmeck, B. Tummeler, et al., Impaired TLR4 and HIF expression in cystic fibrosis bronchial epithelial cells downregulates hemeoxygenase-1 and alters iron homeostasis in vitro, *Am. J. Physiol. Lung Cell Mol. Physiol.* 307 (10) (2014) L791–L799.
- [24] F. Han, W. Gaofeng, S. Han, Z. Li, Y. Jia, L. Bai, X. Li, K. Wang, F. Yang, J. Zhang, et al., Hypoxia-inducible factor prolyl-hydroxylase inhibitor roxadustat (FG-4592) alleviates sepsis-induced acute lung injury, *Respir. Physiol. Neurobiol.* (2020) 103506.
- [25] C. He, W. Zhang, S. Li, W. Ruan, J. Xu, F. Xiao, Edaravone improves septic cardiac function by inducing an HIF-1 α /HO-1 pathway, *Oxid Med Cell Longev* 2018 (2018) 5216383.
- [26] S.L. McHaffie, N.D. Hastie, Y.Y. Chau, Effects of CreERT2, 4-OH tamoxifen, and gender on CFU-F assays, *PLoS One* 11 (2) (2016), e0148105.
- [27] Y. Yang, J. Wang, Y. Li, C. Fan, S. Jiang, L. Zhao, S. Di, Z. Xin, B. Wang, G. Wu, et al., HO-1 signaling activation by pterostilbene treatment attenuates mitochondrial oxidative damage induced by cerebral ischemia reperfusion injury, *Mol. Neurobiol.* 53 (4) (2016) 2339–2353.
- [28] N. Nakamura, Emerging new roles of GM130, a cis-Golgi matrix protein, in higher order cell functions, *J. Pharmacol. Sci.* 112 (3) (2010) 255–264.
- [29] R.M. Hsu, C.Y. Zhong, C.L. Wang, W.C. Liao, C. Yang, S.Y. Lin, J.W. Lin, H. Y. Cheng, P.Y. Li, C.J. Yu, Golgi tethering factor golgin-97 suppresses breast cancer cell invasiveness by modulating NF- κ B activity, *Cell Commun. Signal.* 16 (1) (2018) 19.
- [30] A. Velasco, L. Hendricks, K.W. Moremen, D.R. Tulsiani, O. Touster, M.G. Farquhar, Cell type-dependent variations in the subcellular distribution of alpha-mannosidase I and II, *J. Cell Biol.* 122 (1) (1993) 39–51.
- [31] T. Li, H. You, X. Mo, W. He, X. Tang, Z. Jiang, S. Chen, Y. Chen, J. Zhang, Z. Hu, GOLPH3 mediated Golgi stress response in modulating N2A cell death upon oxygen-glucose deprivation and reoxygenation injury, *Mol. Neurobiol.* 53 (2) (2016) 1377–1385.
- [32] A.A. Waza, Z. Hamid, S. Ali, S.A. Bhat, M.A. Bhat, A review on heme oxygenase-1 induction: is it a necessary evil, *Inflamm. Res.* 67 (7) (2018) 579–588.
- [33] L. Guillot, N. Nathan, O. Tabary, G. Thouvenin, P. Le Rouzic, H. Corvol, S. Amselem, A. Clement, Alveolar epithelial cells: master regulators of lung homeostasis, *Int. J. Biochem. Cell Biol.* 45 (11) (2013) 2568–2573.
- [34] G.L. Semenza, Targeting HIF-1 for cancer therapy, *Nat. Rev. Canc.* 3 (3) (2003) 721–732.
- [35] P. Jaakkola, D.R. Mole, Y.M. Tian, M.I. Wilson, J. Gielbert, S.J. Gaskell, A. von Kriegsheim, H.F. Hebestreit, M. Mukherji, C.J. Schofield, et al., Targeting of HIF-1 α by the von Hippel-Lindau ubiquitylation complex by O₂-regulated prolyl hydroxylation, *Science* 292 (5516) (2001) 468–472.
- [36] W.S. Wang, H.Y. Liang, Y.J. Cai, H. Yang, DMOG ameliorates IFN- γ -induced intestinal barrier dysfunction by suppressing PHD2-dependent HIF-1 α degradation, *J. Interferon Cytokine Res.* 34 (1) (2014) 60–69.
- [37] Q. Yuan, O. Bleiziffer, A.M. Boos, J. Sun, A. Brandl, J.P. Beier, A. Arkudas, M. Schmitz, U. Kneser, R.E. Horsch, PHDs inhibitor DMOG promotes the vascularization process in the AV loop by HIF-1 α up-regulation and the preliminary discussion on its kinetics in rat, *BMC Biotechnol.* 14 (2014) 112.
- [38] M.A. Abou-Seif, A.A. Youssef, Evaluation of some biochemical changes in diabetic patients, *Clin. Chim. Acta* 346 (2) (2004) 161–170.
- [39] J. Djordjevic, A. Djordjevic, M. Adzic, A. Niciforovic, M.B. Radojic, Chronic stress differentially affects antioxidant enzymes and modifies the acute stress response in liver of Wistar rats, *Physiol. Res.* 59 (5) (2010) 729–736.
- [40] S. Samarghandian, M. Azimi-Nezhad, T. Farkhondeh, F. Samini, Anti-oxidative effects of curcumin on immobilization-induced oxidative stress in rat brain, liver and kidney, *Biomed. Pharmacother.* 87 (2017) 223–229.
- [41] T. Sakamoto, H. Imai, Hydrogen peroxide produced by superoxide dismutase SOD-2 activates sperm in *Caenorhabditis elegans*, *J. Biol. Chem.* 292 (36) (2017) 14804–14813.
- [42] N. He, J.J. Jia, H.Y. Xie, J.H. Li, Y. He, S.Y. Yin, R.P. Liang, L. Jiang, J.F. Liu, K. D. Xu, et al., Partial inhibition of HO-1 attenuates HMP-induced hepatic regeneration against liver injury in rats, *Oxid Med Cell Longev* 2018 (2018) 9108483.
- [43] I. Ayala, A. Colanzi, Alterations of Golgi organization in Alzheimer's disease: a cause or a consequence? *Tissue Cell* 49 (2 Pt A) (2017) 133–140.
- [44] T. Li, H. You, J. Zhang, X. Mo, W. He, Y. Chen, X. Tang, Z. Jiang, R. Tu, L. Zeng, et al., Study of GOLPH3: a potential stress-inducible protein from Golgi apparatus, *Mol. Neurobiol.* 49 (3) (2014) 1449–1459.
- [45] H. Alborzina, T.I. Ignashkova, F.R. Dejure, M. Gendarme, J. Theobald, S. Wolf, R. K. Lindemann, J.H. Reiling, Golgi stress mediates redox imbalance and ferroptosis in human cells, *Commun Biol* 1 (2018) 210.
- [46] S. Passemard, F. Perez, P. Gressens, V. El Ghouzi, Endoplasmic reticulum and Golgi stress in microcephaly, *Cell Stress* 3 (12) (2019) 369–384.
- [47] D. Mennerich, S. Kellokumpu, T. Kietzmann, Hypoxia and reactive oxygen species as modulators of endoplasmic reticulum and Golgi homeostasis, *Antioxidants Redox Signal.* 30 (1) (2019) 113–137.
- [48] M. Mancini, C.E. Machamer, S. Roy, D.W. Nicholson, N.A. Thornberry, L. A. Casciola-Rosen, A. Rosen, Caspase-2 is localized at the Golgi complex and cleaves golgin-160 during apoptosis, *J. Cell Biol.* 149 (3) (2000) 603–612.
- [49] K. Nozawa, C.A. Casiano, J.C. Hamel, C. Molinaro, M.J. Fritzler, E.K. Chan, Fragmentation of Golgi complex and Golgi autoantigens during apoptosis and necrosis, *Arthritis Res.* 4 (4) (2002) R3.
- [50] M. Lowe, J.D. Lane, P.G. Woodman, V.J. Allan, Caspase-mediated cleavage of syntaxin 5 and giantin accompanies inhibition of secretory traffic during apoptosis, *J. Cell Sci.* 117 (Pt 7) (2004) 1139–1150.
- [51] J.D. Lane, J. Lucocq, J. Pryde, F.A. Barr, P.G. Woodman, V.J. Allan, M. Lowe, Caspase-mediated cleavage of the stacking protein GRASP65 is required for Golgi fragmentation during apoptosis, *J. Cell Biol.* 156 (3) (2002) 495–509.
- [52] S.J. Guiney, P.A. Adlard, A.I. Bush, D.I. Finkelstein, S. Aytton, Ferroptosis and cell death mechanisms in Parkinson's disease, *Neurochem. Int.* 104 (2017) 34–48.
- [53] M.M. Gaschler, B.R. Stockwell, Lipid peroxidation in cell death, *Biochem. Biophys. Res. Commun.* 482 (3) (2017) 419–425.
- [54] C. Liu, M. Mei, Q. Li, P. Roboti, Q. Pang, Z. Ying, F. Gao, M. Lowe, S. Bao, Loss of the golgin GM130 causes Golgi disruption, Purkinje neuron loss, and ataxia in mice, *Proc. Natl. Acad. Sci. U. S. A.* 114 (2) (2017) 346–351.
- [55] J. Weidner, L. Jarenback, I. Aberg, G. Westergren-Thorsson, J. Ankerst, L. Bjerner, E. Tuvfesson, Endoplasmic reticulum, Golgi, and lysosomes are disorganized in

- lung fibroblasts from chronic obstructive pulmonary disease patients, *Phys. Rep.* 6 (5) (2018).
- [56] R.S. Kuna, S.J. Field, GOLPH3: a Golgi phosphatidylinositol(4)phosphate effector that directs vesicle trafficking and drives cancer, *J. Lipid Res.* 60 (2) (2019) 269–275.
- [57] K.N. Yu, H.J. Kim, S. Kim, O. Dawaadamdin, A.Y. Lee, S.H. Hong, S.H. Chang, S. J. Choi, S.M. Shim, K. Lee, et al., Cigarette smoking condensate disrupts endoplasmic reticulum-golgi network homeostasis through GOLPH3 expression in normal lung epithelial cells, *Nicotine Tob. Res.* 18 (9) (2016) 1877–1885.
- [58] K. Raghavendran, L.M. Napolitano, ALI and ARDS: challenges and advances, *Crit. Care Clin.* 27 (3) (2011) xiii-xiv.
- [59] P. Kosutova, P. Mikolka, M. Kolomaznik, S. Balentova, M. Adamkov, A. Calkovska, D. Mokra, Reduction of lung inflammation, oxidative stress and apoptosis by the PDE4 inhibitor roflumilast in experimental model of acute lung injury, *Physiol. Res.* 67 (Supplementum 4) (2018) S645–S654.
- [60] S.K. Kim, S.J. Rho, S.H. Kim, S.Y. Kim, S.H. Song, J.Y. Yoo, C.H. Kim, S.H. Lee, Protective effects of diphenyleioidonium, an NADPH oxidase inhibitor, on lipopolysaccharide-induced acute lung injury, *Clin. Exp. Pharmacol. Physiol.* (2018).
- [61] S.R. Kim, H.J. Kim, D.I. Kim, K.B. Lee, H.J. Park, J.S. Jeong, S.H. Cho, Y.C. Lee, Blockade of interplay between IL-17a and endoplasmic reticulum stress attenuates LPS-induced lung injury, *Theranostics* 5 (12) (2015) 1343–1362.
- [62] J. Shi, J.B. Yu, W. Liu, D. Wang, Y. Zhang, L.R. Gong, S.A. Dong, D.Q. Liu, Carbon monoxide alleviates lipopolysaccharide-induced oxidative stress injury through suppressing the expression of Fis1 in NR8383 cells, *Exp. Cell Res.* 349 (1) (2016) 162–167.